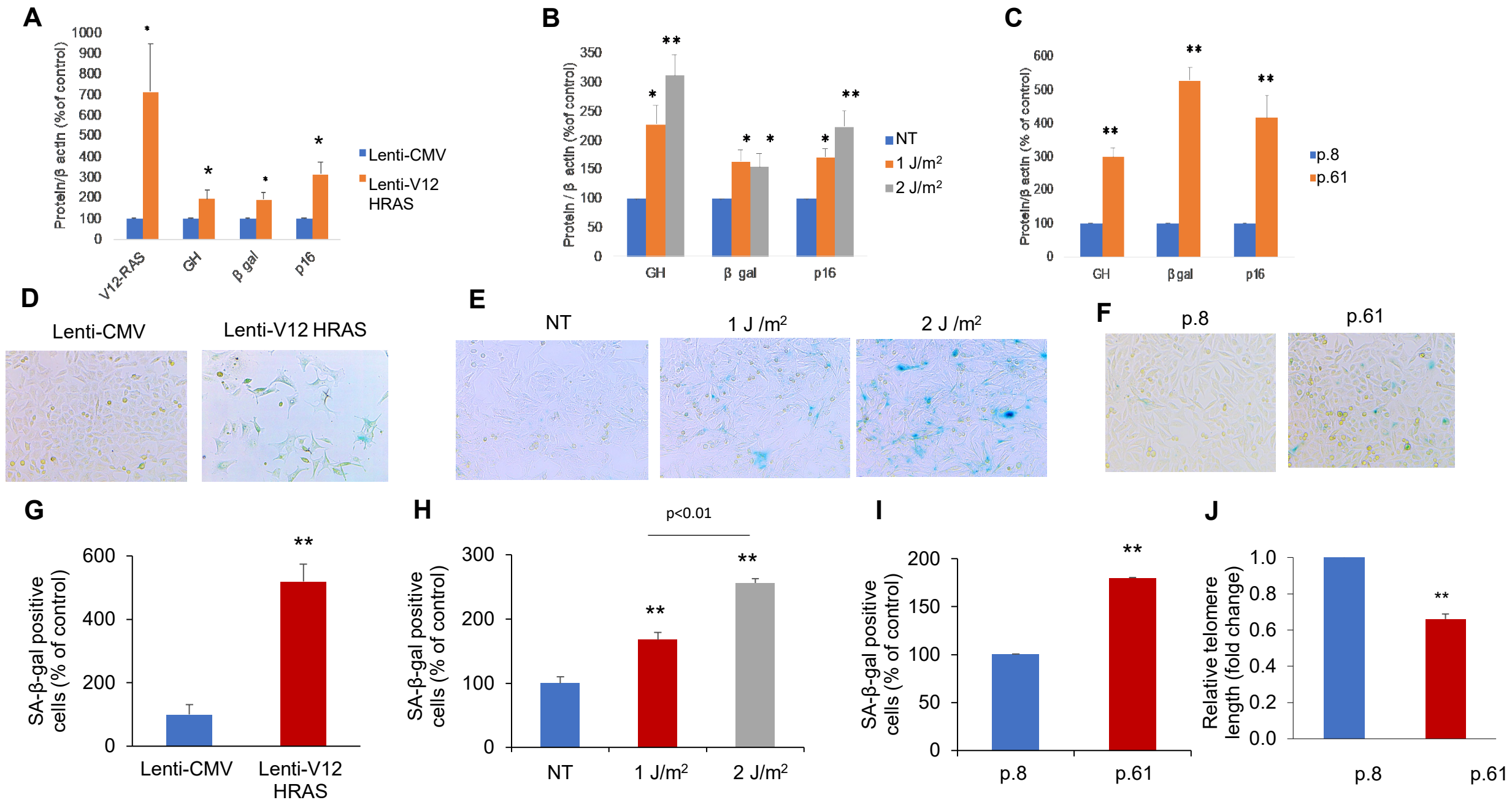


# **Non-pituitary growth hormone enables colon cell senescence evasion**

Vera Chesnokova, Svetlana Zonis, Tugce Apaydin, Robert Barrett, Shlomo Melmed

## **Supplemental Information**



**Figure S1**

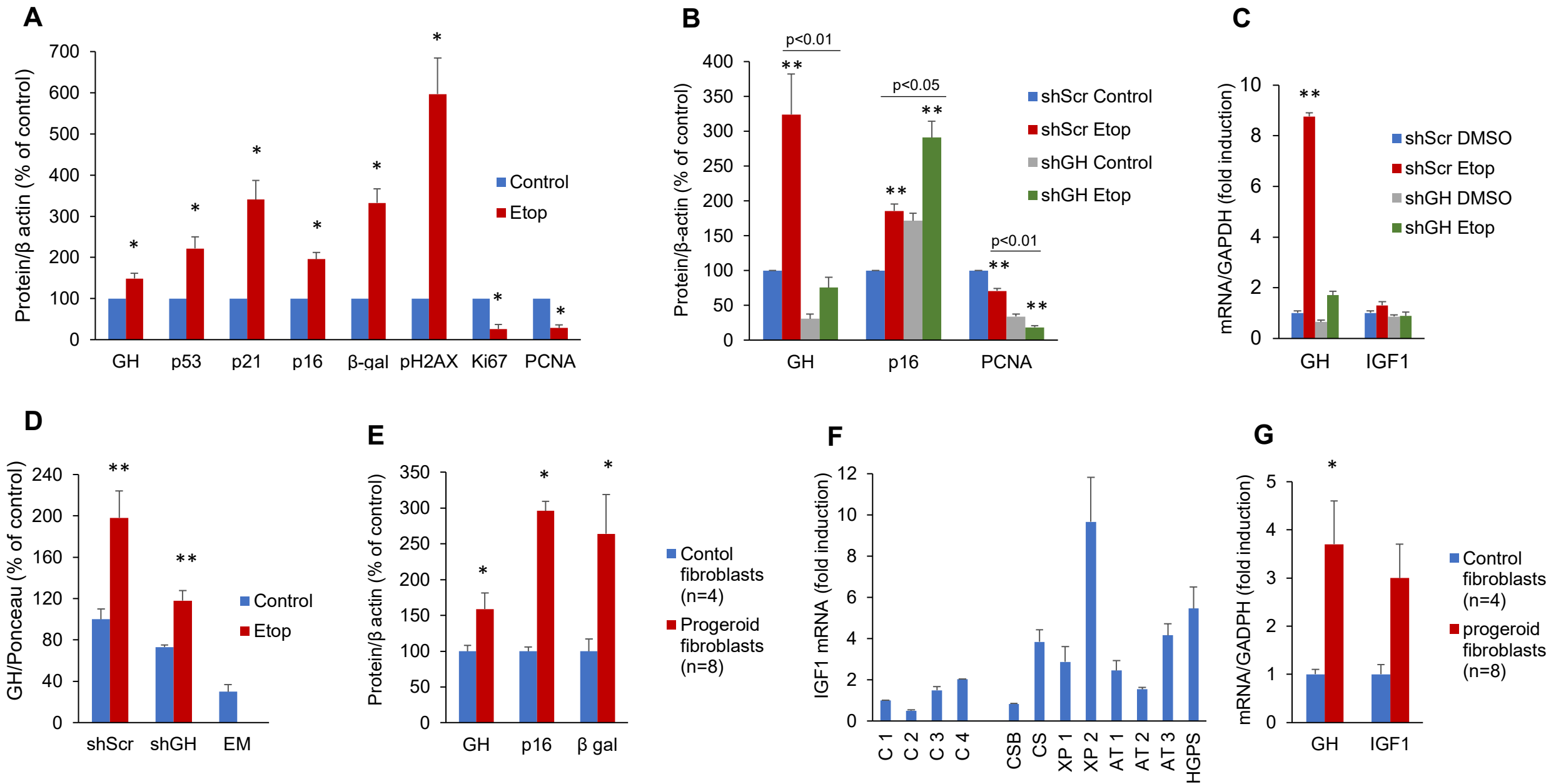


Figure S2

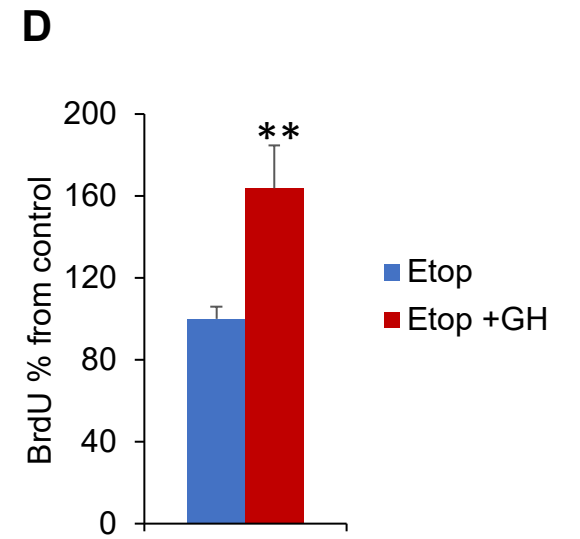
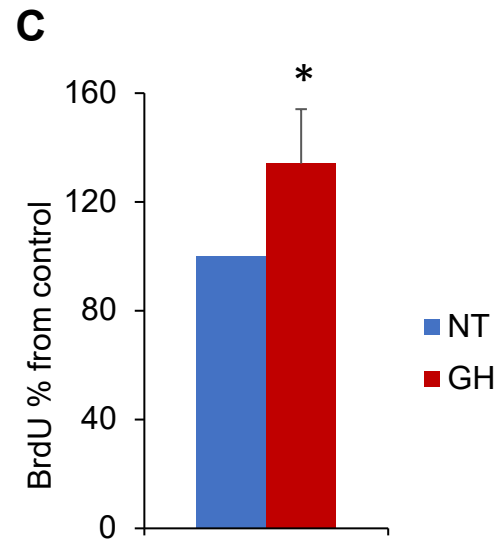
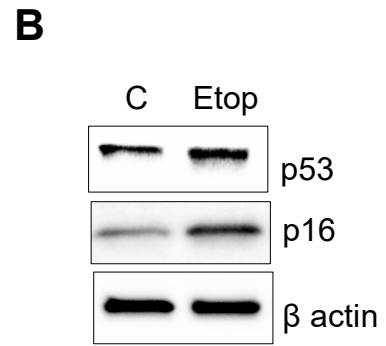
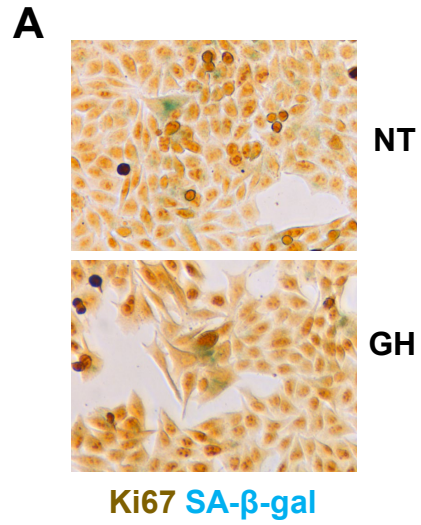


Figure S3

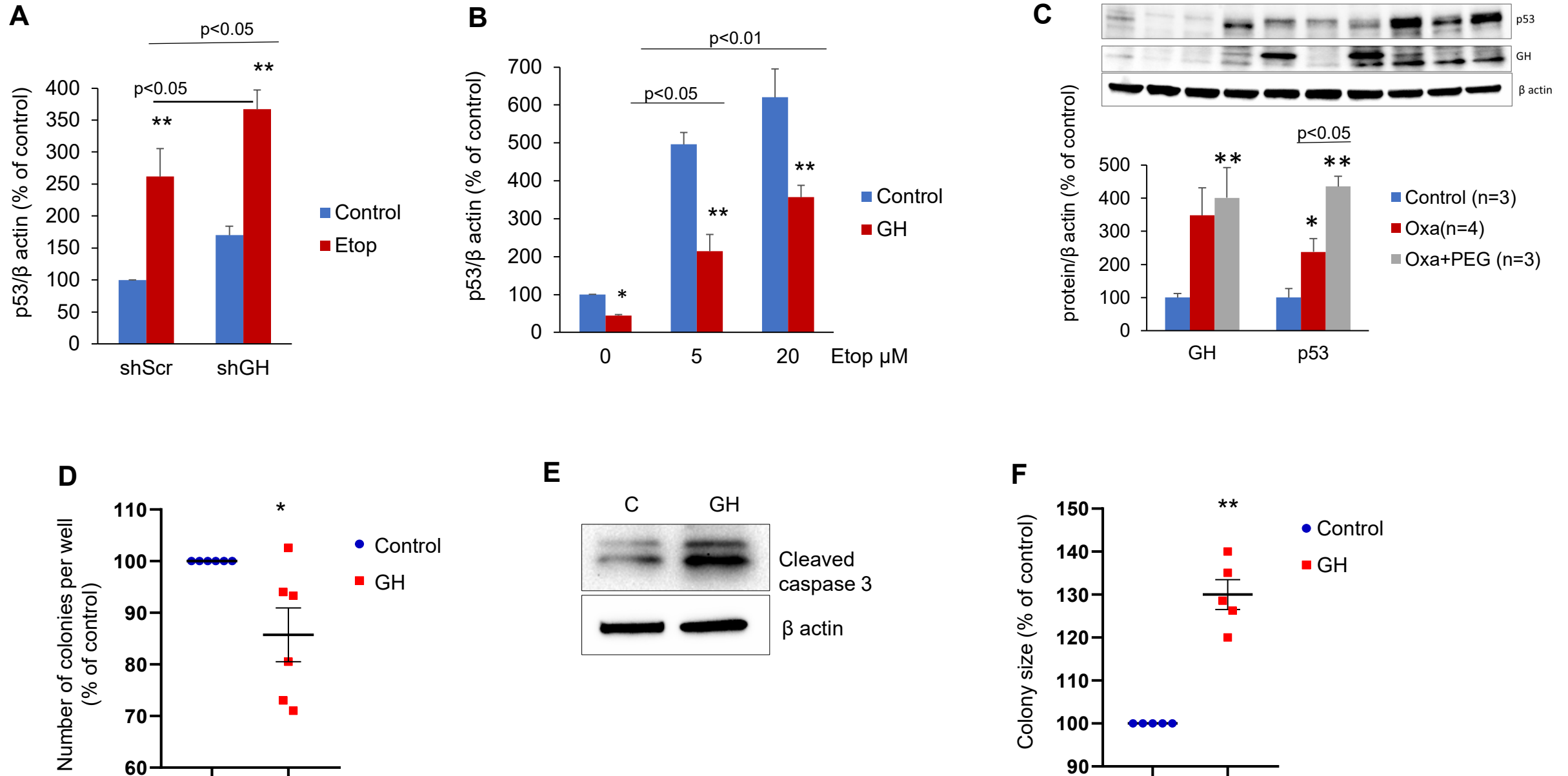
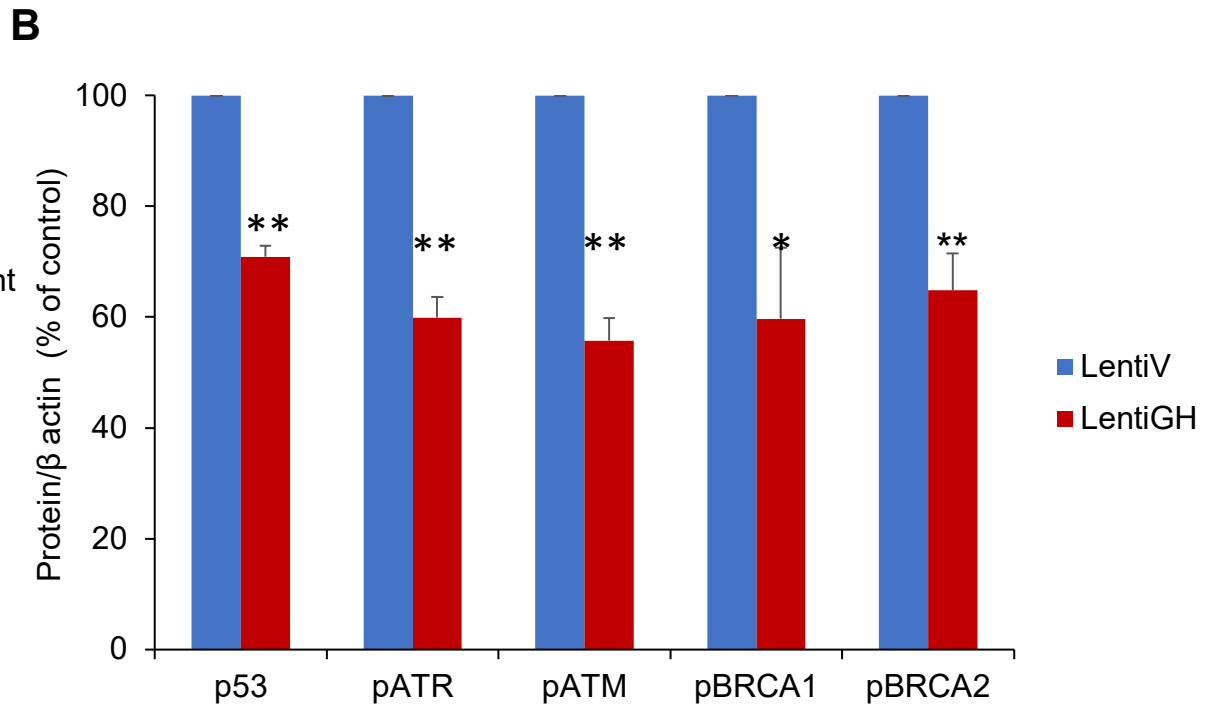
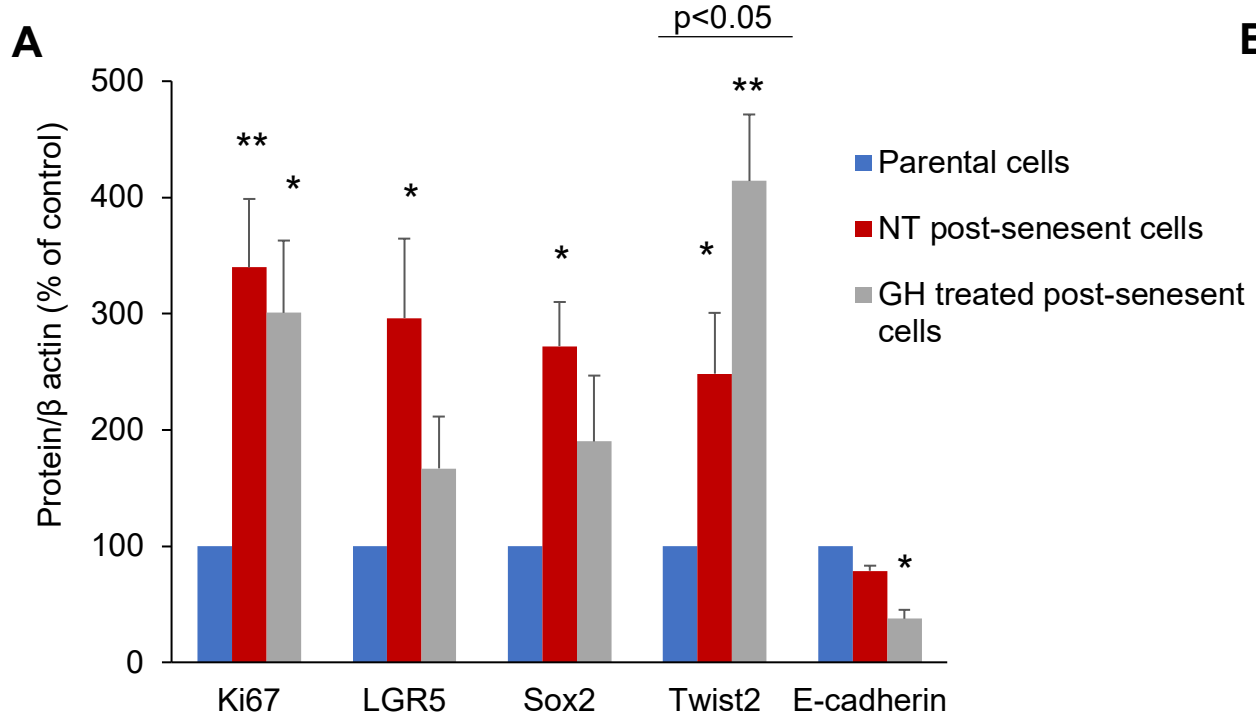
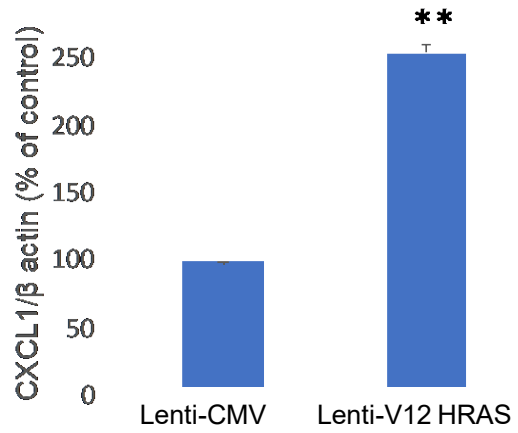
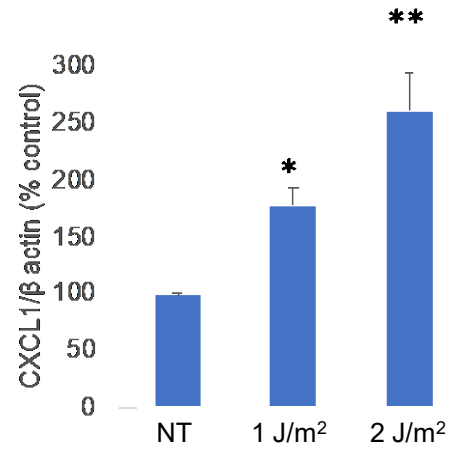
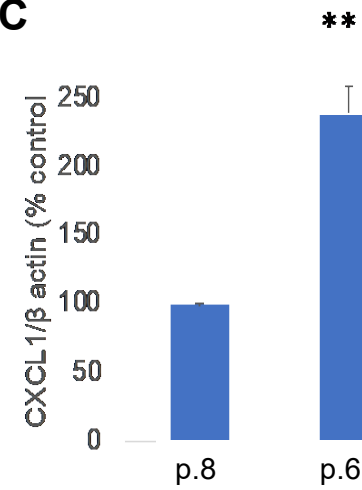
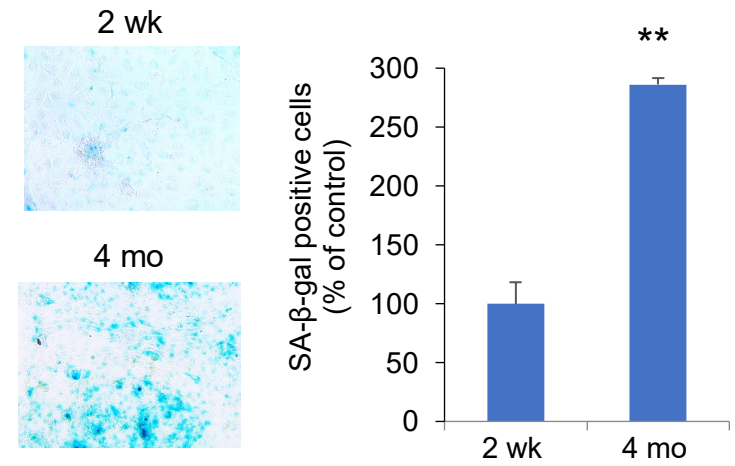
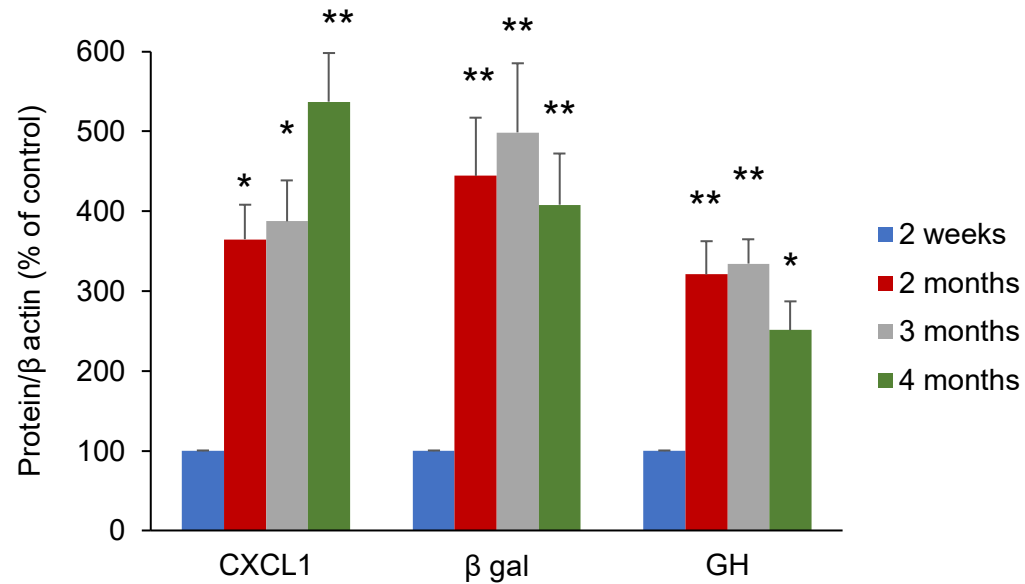
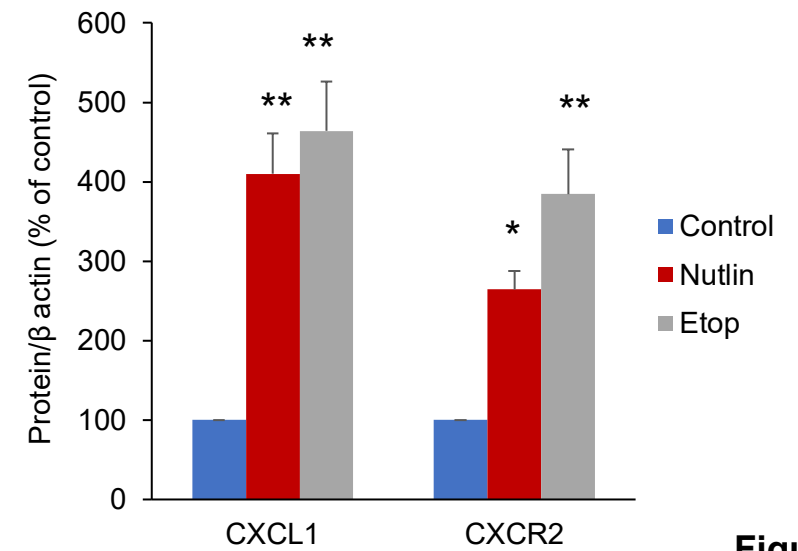
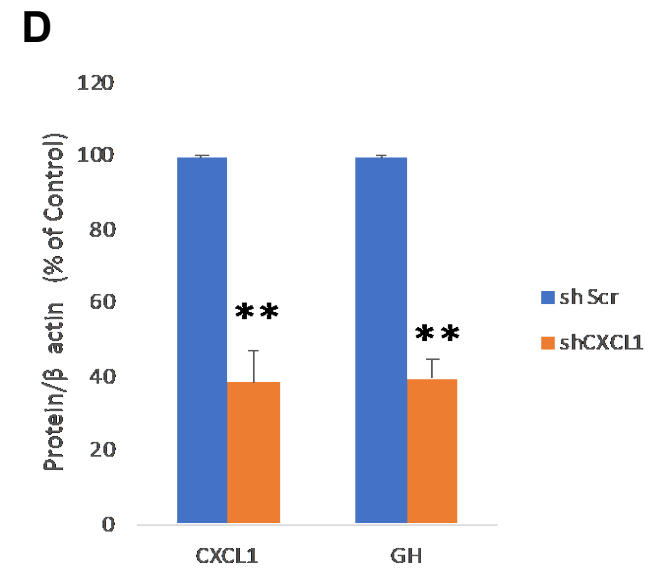
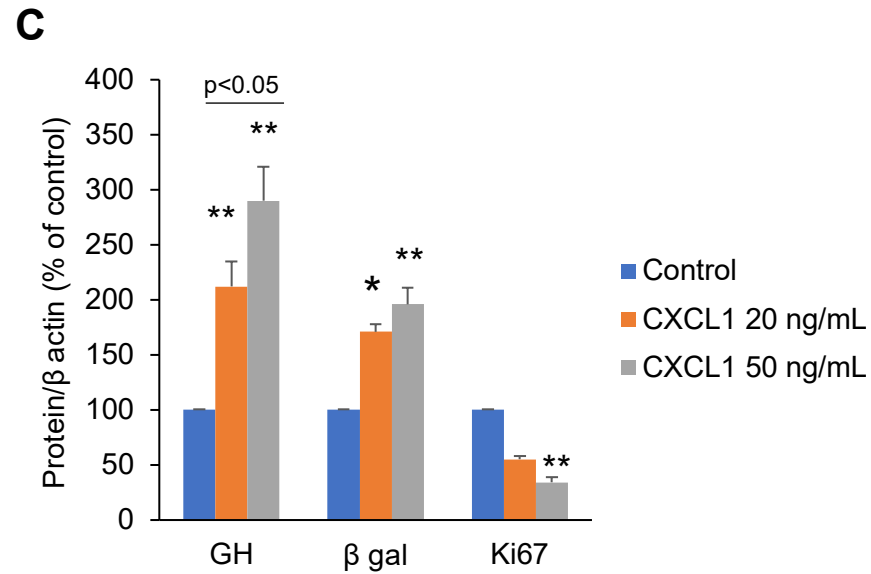
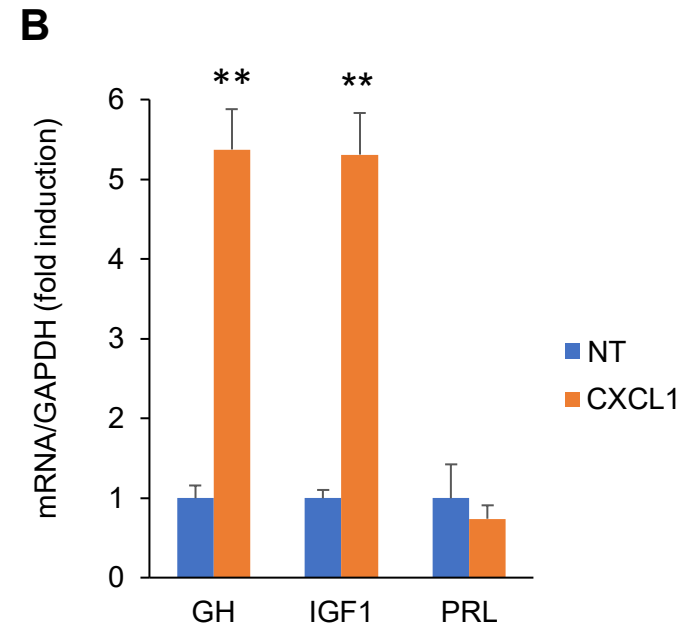
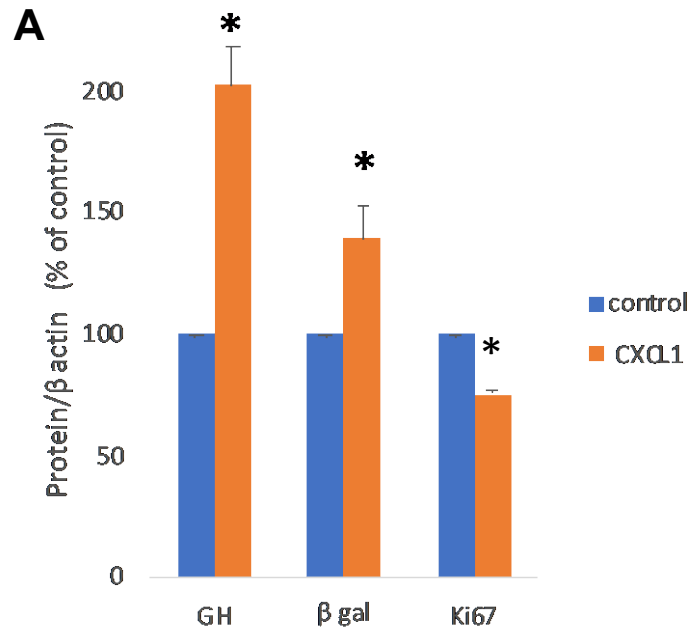


Figure S4



**Figure S5**

**A****B****C****D****E****F****Figure S6**



**Figure S7**



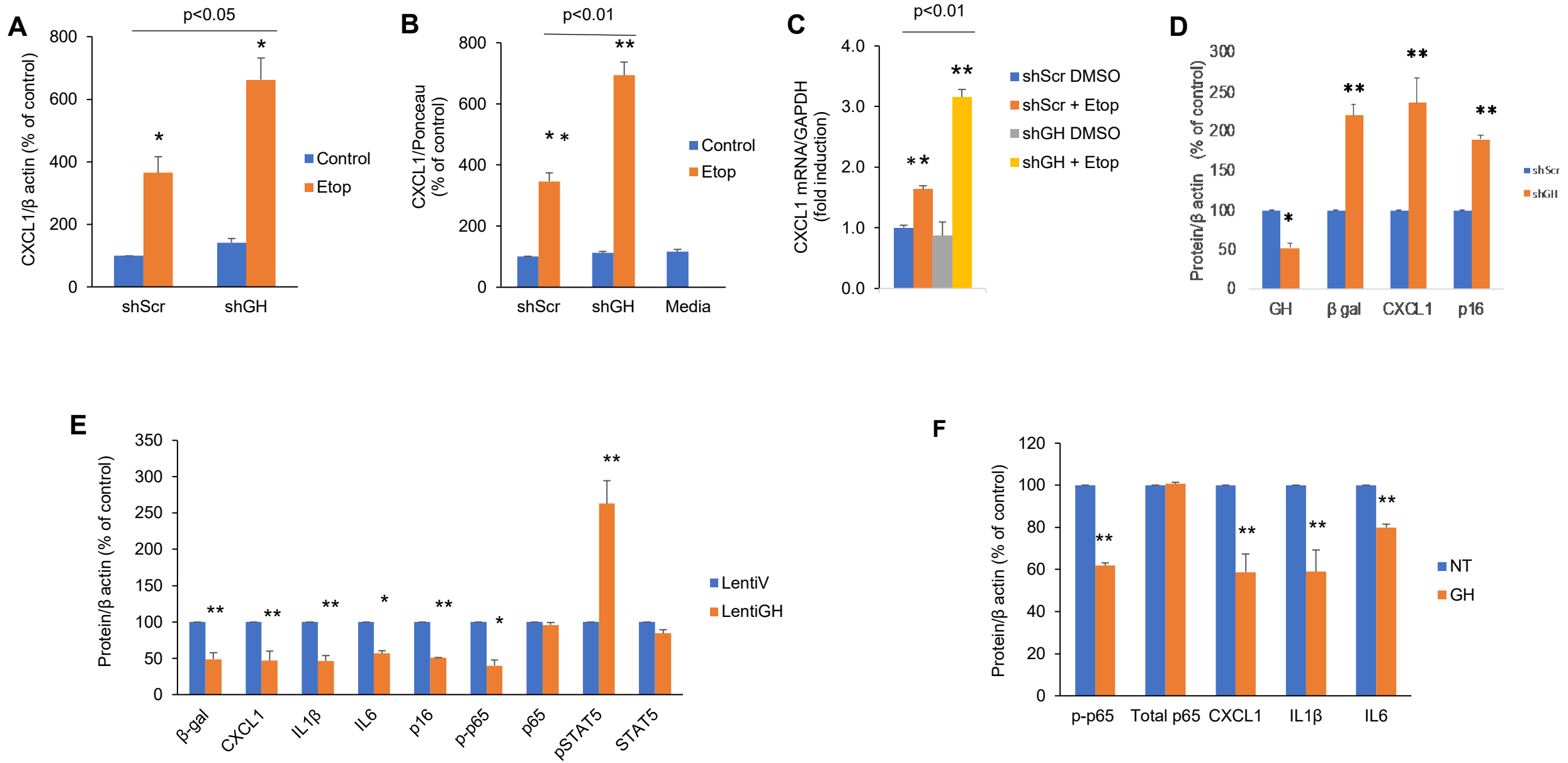
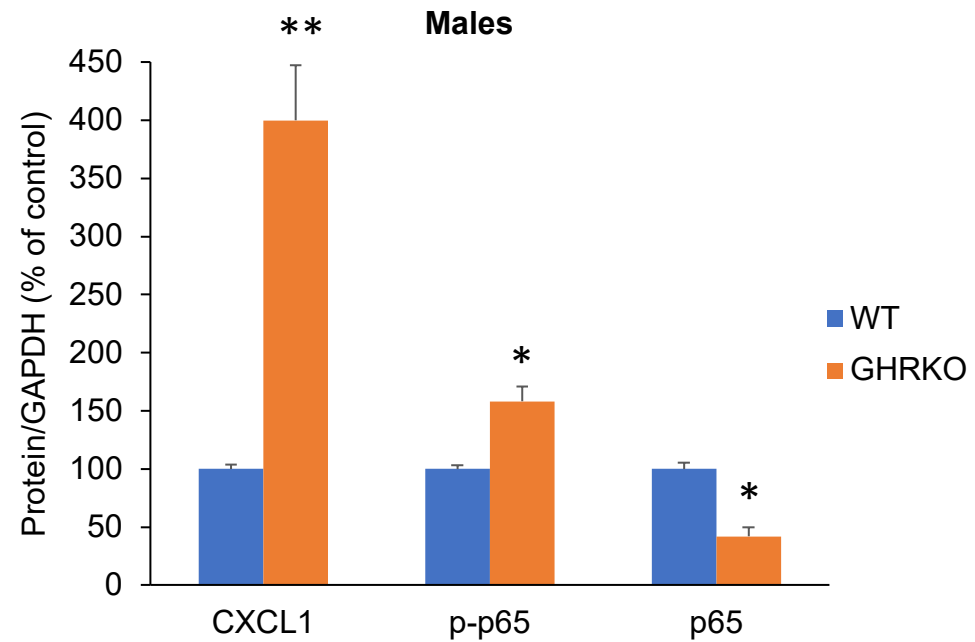
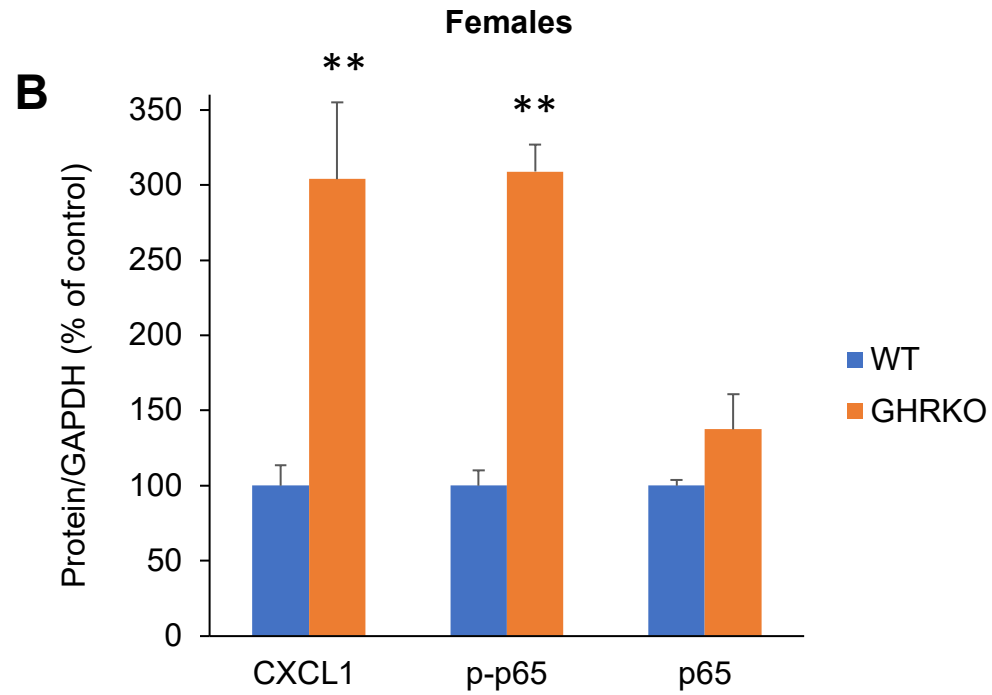
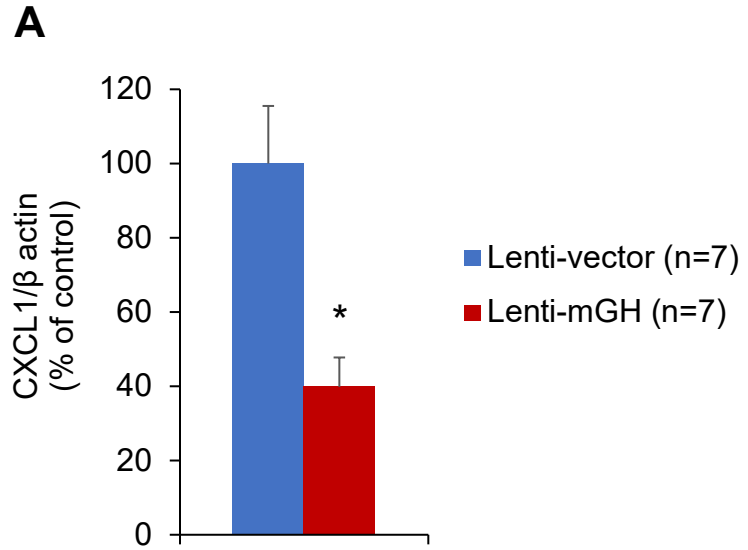


Figure S8



**Figure S9**

	<i>Number of tumors observed</i>				<b>Average tumor size (mm)</b>
	<b>Spleen</b>	<b>Liver</b>	<b>Peritoneum</b>	<b>Total Tumors</b>	
<b>HCT116 lenti-Vector (n=8)</b>	4	0	2	6	1.33 ± 0.18
<b>HCT116 lenti-hGH (n=8)</b>	7	4	16	27	2.85 ± 0.43

**Table S1**

## Supplement Figures Legends

**Figure S1. GH is induced in different senescence models. (A-C)** ImageJ quantification of GH and senescence markers in hNCC. (A) Oncogene-induced senescence. Cells were infected with lentivirus expressing constitutively activated HRAS oncogene (lentiV-12RAS) or empty vector (lenti-CMV) and analyzed 7 days later. (C) Replicative senescence. (B) DNA damage-induced senescence. Cells were exposed to UVC light at indicated doses or left untreated (NT) and analyzed 6 days later. Cells were passaged until proliferation was exhausted. Cells from passage 8 (p.8) and passage 61 (p.61) were compared. **(D-F)** Representative images of SA- $\beta$ -gal expression in each senescence model. **(G-I)** Number of SA- $\beta$ -gal-positive cells depicted as percent of control in each senescence model. At least 5 fields were analyzed. **(J)** Telomere length assay showing telomere shortening with prolonged culturing, as a reflection of aging. The results shown as mean  $\pm$  SEM. In A,C,G,I,J the differences from control were analyzed by two-tail Student's t-test. In B, the differences were analyzed by two-way ANOVA, and in H by one-way ANOVA followed by ad-hoc Tukey's test to adjust for multiple comparisons. In A-C and G-I, results are graphed as percent of control, but statistical testing was performed on raw numbers. \*,  $p < 0.05$ ; \*\*,  $p < 0.01$  vs comparator.

**Figure S2. GH is induced in senescent cells and is a SASP component. (A)** ImageJ quantification of senescence markers in hNCC treated with 50  $\mu$ M etoposide (Etop) or DMSO for 48h, and analyzed 7 days after beginning treatment. **(B)** Western blot of GH, p16 and PCNA expression and **(C)** Real time PCR results of GH and IGF1 in hNCC stably infected with lenti shScr (as control) or lenti shGH and treated with 50  $\mu$ M

etoposide (Etop) or DMSO for 48h, and grown for an additional 4 days. In C, results are expressed as fold-change vs control (shScr DMSO treated) taken as 1. Results are shown as mean  $\pm$  SEM of triplicate measurements. **(D)** ImageJ quantification of secreted GH in culture medium. EM, empty medium. **(E-G)** Senescent markers and IGF1mRNA in fibroblasts derived from patients with progeroid syndrome and healthy volunteers (control). **(E)** ImageJ quantification of senescence markers. **(F)** Real-time PCR of IGF1 mRNA. **(G)** The average of GH and IGF1 mRNA levels from fibroblasts derived from patients with progeroid syndrome and healthy volunteers (control). Real-time PCR results are shown as mean  $\pm$  SEM of triplicate measurements and expressed as fold-change vs control taken as 1. AT, ataxia telangiectasia; CS, Cockayne syndrome; CSB, Cockayne syndrome group B; HGPS, Hutchinson-Gilford progeroid syndrome; XP, xeroderma pigmentosa. Results are shown as mean  $\pm$  SEM of triplicate measurements. In B and D, differences were analyzed by two-way ANOVA followed by ad-hoc Tukey's test to adjust for multiple comparisons. In A,E,G differences from control were analyzed by two-tailed Student's t test. In A,B,D,E proteins are normalized to loading control and graphed as percent of control, but statistical testing was performed on raw numbers. \*,  $p < 0.05$ ; \*\*,  $p < 0.01$  vs comparator.

**Figure S3. GH triggers proliferation in senescent cells.** **(A)** Representative images of non-senescent parental hNCC not treated (NT) and treated with GH only. Ki67 (brown) expression in senescent (blue) SA- $\beta$ -gal-positive cells. Cells treated with etoposide only or with etoposide and GH are depicted in Figure 2A. **(B)** Senescence markers of hNCC treated with 50  $\mu$ M etoposide for 48 hours and analyzed 6 days after beginning treatment. **(C)** BrdU incorporation. hNCC that reached replicative

senescence (p.61) were treated with 500 ng/mL GH or left untreated (NT) and analyzed 24h later. **(D)** BrdU incorporation in senescent cells treated with 50  $\mu$ M etoposide for 48h to induce senescence, then with 500 ng/mL GH for 24h. In C,D results are shown as mean  $\pm$  SEM of 3 independent experiments and analyzed with two-tail Student test. \*,  $p < 0.05$  control.

**Figure S4. GH suppresses p53 in senescent cells and affects colony**

**formation. (A-B)** ImageJ quantification of p53 in (A) hNCC infected with either lenti-shScr as control or lenti-shGH, treated with 50  $\mu$ M etoposide (Etop) or left untreated (Control) for 48h, and grown for an additional 4 days; and (B) hNCC pre-treated with 500 ng/mL GH and indicated doses of etoposide, then analyzed 24h later. Results are shown as mean  $\pm$  SEM of at least 3 replicate measurements normalized to loading control. Differences were analyzed in A by one-way ANOVA and in B by two-way ANOVA followed by ad-hoc Tukey's test to adjust for multiple comparisons. **(C)** Western blot of GH and p53 in colon tissue of hypophysectomized rats after 5 injection of either Oxaliplatin (Oxa) (i.p. 4 mg/kg) alone or oxaliplatin with pegvisomant (PEG) (s.q. 0.57 mg/kg). Lower panel: ImageJ quantification of GH and p53. For (A-C) C, control. **(D-F)** hNCC were pretreated with 50  $\mu$ M etoposide for 48h, sorted for senescence, and cultured in the presence of 500 ng/mL GH 10 days after plating. (D) Number of colonies per well. (E) Western blot of cleaved caspase 3. (F) Colony size. One dot represents one experiment. In C and E, results are shown as mean  $\pm$  SEM. In C, D and F results were analyzed by two tailed Student's t test. Results are graphed as percent of control, but statistical testing was performed on raw numbers. \*,  $p < 0.05$ ; \*\*,  $p < 0.01$  vs control.

**Figure S5. Paracrine GH triggers proliferation and EMT and suppresses DNA damage pathway. (A)** ImageJ quantification of proliferation, stemness, and EMT markers in hNCC line #1 treated with 50  $\mu$ M etoposide, sorted for senescence 7 days later, and cultured for 10 days in the presence of or absence of GH; cells were then sorted again for SA- $\beta$ -gal positivity. Only SA- $\beta$ -gal negative (post-senescent cells) were analyzed. **(B)** Organoids were infected with lentiV or lentiGH (both expressing GFP) and cultured for 5 weeks; organoid cells were then sorted for GFP-positive and GFP-negative expression and only GFP-negative cells co-cultured with either lentiV or lentiGH organoid cells were analyzed. ImageJ quantification of DNA damage and repair proteins shown. In A and C, results are shown as mean  $\pm$  SEM of triplicate measurements normalized to loading control. In A, results were analyzed by one-way ANOVA followed by ad-hoc Tukey's test to adjust for multiple comparisons. In C, results were analyzed by two-tailed Student's t-test. Results are graphed as percent of control, but statistical testing was performed on raw numbers. \*,  $p < 0.05$ ; \*\*,  $p < 0.01$  vs comparator.

**Figure S6. CXCL1 is induced in senescent cells. (A-C)** Image J quantification of CXCL1 in different models of senescence. (A) Oncogene-induced senescence. Cells were infected with lentivirus expressing constitutively activated HRAS oncogene (lentiV12HRAS) or empty vector (lentiV-CMV) and analyzed 7 days later. (B) DNA damage induced senescence. Cells were exposed to indicated doses of UVC light or left untreated (NT) and analyzed 6 days later. (C) Replicative senescence. Cells were passaged until proliferation was significantly reduced. Cells from passage 8 (p.8) and passage 61 (p.61) were compared. In all experiments, CXCL1 expression was normalized

to the same loading control as in Figures 1A, 1B, and 1C, respectively. (D) SA- $\beta$ -gal enzymatic activity in human intestinal organoids cultured for 2 weeks and 4 months. Representative images and number of SA- $\beta$ -gal–positive cells depicted as percent of control. Six fields/experiment were counted. Results are shown as mean  $\pm$  SEM. (E) ImageJ quantification of senescent organoid proteins cultured for up to 4 months. (F) ImageJ quantification of CXCL1 and its receptor CXCR2 in hNCC 72h after treatment with either 3  $\mu$ M nutlin3 (Nutlin) or 5  $\mu$ M etoposide (Etop) for 48h or left untreated (Control, C). In A-F, results are shown as mean  $\pm$  SEM normalized to loading control. In A,C,D differences between cultures was analyzed with two-tailed Student's t-test. In B,E,F differences were analyzed by one-way ANOVA followed by ad-hoc Tukey's test to adjust for multiple comparisons. Results are graphed as percent of control, but statistical testing was performed on raw numbers. \*,  $p < 0.05$ ; \*\*,  $p < 0.01$  vs comparator.

**Figure S7. CXCL1 induces GH expression.** (A) ImageJ quantification of proteins from organoids treated with 100 ng/mL CXCL1 for 96h. (B) Real-time PCR of senescent organoids treated with CXCL1 for 96h. Experiment was repeated 3 times. In A and B, differences with control (NT) were analyzed with two-tailed Student's t-test. In B, results are shown as mean  $\pm$  SEM of triplicate measurements, expressed as fold-change vs control taken as 1. (C) ImageJ quantification of hNCC treated with indicated doses of CXCL1 for 96h. (D) ImageJ quantification of hNCC infected with lenti-shCXCL1 or lenti-shScr and analyzed 3 days after infection. In C and D, results were analyzed by one- and two-way ANOVA, respectively, followed with ad-hoc Tukey's test to adjust for multiple comparisons. Results are shown as mean  $\pm$  SEM of at least 3 replicate measurements normalized to loading controls. Results are graphed as percent of



control, but statistical testing was performed on raw numbers. \*,  $p < 0.05$ ; \*\*,  $p < 0.01$  vs comparator.

**Figure S8. GH suppresses CXCL1 expression and secretion in senescent cells.** (A-C) hNCC were infected with either lenti-shGH or lenti-shScr, treated with 50  $\mu\text{M}$  etoposide (Etop) to induce senescence for 48h or left untreated (C) and analyzed 6 days later. (A) ImageJ quantification of CXCL1 in cells. (B) ImageJ quantification of CXCL1 in culture medium. (C) Real-time PCR of CXCL1 mRNA. In A-C, differences with respective controls were analyzed by two-way ANOVA followed by ad-hoc Tukey's test to adjust for multiple comparisons. Results are shown as mean  $\pm$  SEM of triplicate measurements and in C are depicted as fold-change vs control taken as 1. (D) ImageJ quantification of proteins in organoids 1 week after infection with lenti-shGH or lenti-shScr. (E) ImageJ quantification of proteins in organoids 1 week after infection with lentiGH or lentiV. (F) Image J quantification of proteins in hNCC treated with 50  $\mu\text{M}$  etoposide for 2 days, sorted for senescence on day 3, and treated with GH for an additional 24h. Results are shown as mean  $\pm$  SEM of triplicate measurements normalized to loading control. In D-F, results were analyzed by two-tailed Student's t-test. Results are graphed as percent of control, but statistical testing was performed on raw numbers. \*,  $p < 0.05$ ; \*\*,  $p < 0.01$  vs comparator.

**Figure S9. GH suppresses CXCL1 and GH deficiency upregulates CXCL1 in vivo.** (A) GH suppresses CXCL1 in vivo. ImageJ quantification of CXCL1 in colon tissue from female nude mice implanted with HCT116 GH-secreting xenografts (lenti-mGH) or empty vector (lenti-V) and sacrificed 5 weeks later. (B) GH signaling deficiency results

in CXCL1 upregulation in vivo. ImageJ quantification of CXCL1, p-p65, and p65 in colon tissue of female and male GHR knockout (GHRKO) and wild-type (WT) mice. Results are shown as mean  $\pm$  SEM normalized to loading control, assessed using two-tailed Student's t test. \*,  $p < 0.05$ ; \*\*,  $p < 0.01$  vs control.

**Table S1.** Metastatic lesions developed in Nu/J mice carrying GH-secreting (lentiGH) or control vector-expressing (lentiV) xenografts 4 weeks after intrasplenic injection of post-senescent hNCC.